Local composition heterogeneities occurring during crystallization in PVF_2/PMMA blends as studied by high-resolution solid-state ^{13}C n.m.r.

Piotr Tékély*, Françoise Laupretre and Lucien Monnerie
Laboratoire de Physico-Chimie Structurale et Macromoléculaire associé au C.N.R.S., E.S.P.C.I., 10 rue Vauquelin, 75231 Paris Cedex 05, France
(Received 14 June 1984; revised 26 October 1984)

High-resolution solid-state ^{13}C n.m.r. has been used to study the amorphous phase of PVF_2/PMMA blends. The decrease of the carbon magnetization as a function of the contact duration in a cross-polarization sequence was analysed in terms of the local composition heterogeneities occurring during PVF_2 crystallization. The influence of the composition and thermal history of the samples is discussed.

(Keywords: poly(vinyl fluoride); poly(methyl methacrylate); blends; semi-crystalline polymer blends; nuclear magnetic resonance; crystallization; piezoelectric polymers)

INTRODUCTION

Blends of poly(vinylidene fluoride) (PVF_2) and poly(methyl methacrylate) (PMMA) are known to be compatible over a wide range of compositions. Their miscibility in the bulk state has been established according to a number of different criteria such as the observation of one glass transition temperature, or the lowering of the melting temperature. Different techniques were used such as d.s.c.[1-4], dilatometry[1], mechanical relaxation[5], microscopy[6], infra-red[7] and X-ray[6,8] spectroscopies. These techniques test the miscibility and structure of the blends over characteristic lengths ranging from microns to angstroms. The PVF_2/PMMA blends were also studied by n.m.r. methods sensitive to short-range interactions. Douglass and McBrierty[9], using conventional T_1, $T_{1\rho}$, and T_2 measurements for ^{19}F resonance and transient Overhauser experiments over a large temperature range, concluded that a substantial fraction of PVF_2 molecules in the amorphous regions have PMMA chains at near-neighbouring distances, which is evidence for a substantial degree of intimate mixing of PVF_2 and PMMA on a molecular scale. Recently Lin and Ward[10] have used high-resolution solid-state ^{13}C n.m.r. to study PVF_2/PMMA blends. On the basis of the observed intensity attenuations of carbon signals, they also drew the conclusion of the miscibility of the system on a molecular level.

However, in the case of these blends, in which one of the two components (PMMA) is an amorphous polymer whereas the latter (PVF_2) is crystallizable, questions arise as to the precise composition of the amorphous phase of the blends as well as to the heterogeneities that occur during the PVF_2 crystallization process. An extensive study of such a problem was investigated by Stein and coworkers[11] who examined the blends of poly((ε-caprolactone) with poly(vinyl chloride) in the solid state by low-angle X-ray and small-angle light scattering. Because of the crystallinity of poly (ε-caprolactone), these workers not only had to describe the local order and the molecular distribution within the amorphous structures, but also had to determine the spherulite size, the repeat period of the lamellar structures, and the thickness of the crystalline region in relation to the amorphous layers.

In the case of PVF_2/PMMA blends, the degree of crystallinity of the mixtures was determined by *FT*i.r. analysis[12]. According to their composition, samples were shown to be either amorphous when the content of PVF_2 is low, or partly crystalline for higher PVF_2/PMMA ratios, the exact value of the degree of crystallinity being dependent on the thermal treatment. The work of Stein and coworkers[11] on poly(ε-caprolactone) was mainly focused on the crystal phase nature and on crystallization kinetics. Indeed, until now, no information concerning the precise nature and homogeneity of the amorphous phase of binary blends involving amorphous and crystallizable components has been obtained. This deeper insight can be produced by high-resolution solid-state ^{13}C n.m.r.

The first study of blends by high-resolution solid-state ^{13}C n.m.r. was the work of Schaefer and coworkers on poly(phenylene oxide)/polystyrene[13] and polystyrene/polybutadiene block copolymer[14] blends. As shown by Schaefer[15], the high resolution of the ^{13}C n.m.r. experiment can be employed to measure individual spin-lattice relaxation times in the rotating frame for protons attached to different kinds of carbons. This is possible because the final evolution of the carbon signal intensity, as a function of the contact time in a cross-polarization experiment, is governed by the proton spin-lattice relaxation time in the rotating frame $T_{1\rho}$. Through the spin-diffusion relaxation mechanism[16], proton spin-lattice relaxation rotating frame parameters are strongly dependent on short-range spatial proximity of the interacting dipole moments of protons and thus are very sensitive to the homogeneity of the blend.

In the present paper, this type of experiment is used to provide information on the morphological features of PVF_2/PMMA blends and on their dependence on composition and thermal history.

EXPERIMENTAL

The mixtures of PVF_2/PMMA with different weight ratios were supplied by Solvay. Samples were compression moulded at 463 K for 10 min and quenched in an

* On leave from the Institute of Polymer Chemistry, Polish Academy of Sciences, Zabrze, Poland.

0032-3861/85/071081-06$03.00

ice–water bath. The conditions of subsequent thermal treatment of some blends are described in detail in the text.

^{13}C cross-polarization, proton dipolar decoupling and magic-angle spinning (CP/DD/MAS) n.m.r. experiments were performed at 75.47 MHz on a Bruker CXP 300 spectrometer, employing quadrature detection and a single r.f. coil, which is double-tuned for both ^{13}C and ^{1}H. The cross-polarization pulse sequence used in the experiments is shown in *Figure 1*. The matched spin-lock cross-polarization transfers employed ^{13}C and ^{1}H magnetic field strengths of 50 kHz. The proton spin-lattice relaxation times in the rotating frame $T_{1\rho}$ were obtained from a plot of the relative magnitude of the carbon magnetization as a function of the carbon–proton contact duration. In all the spectra, spin-temperature inversion techniques were employed to minimise base line noise and roll[17]. Flip-back[18] was also systematically used to shorten the delay time between two successive pulse sequences. Spinning experiments at the magic-angle using boron nitrure and PMMA-d8 rotors were performed with 3.5 kHz spinning speeds. According to the blend composition 300 to 2000 scans were needed to obtain a good signal-to-noise ratio.

RESULTS AND DISCUSSION

^{13}C n.m.r. spectra

The ^{13}C CP/DD/MAS n.m.r. spectrum of PMMA is given in *Figure 2a*. For comparison a ^{13}C stick spectrum of PMMA in solution is shown in *Figure 2b*[19–21]. The agreement between the resonance positions in solution and in the solid-state is good. Clearly, in the solid-state, the fine structures due to the different microstructures are not resolved. Only the α-methyl carbon resonance is somewhat asymmetric due to a dispersion of chemical shifts arising from stereochemical differences within the chain. In general, a non-resolved fine structure due to tacticity effects is the main cause of line broadening[21].

The ^{13}C CP/DD/MAS spectrum of PVF_2 is plotted in *Figure 2c*. For comparison a high-resolution ^{13}C spectrum of the resonances of PVF_2 in solution, with simultaneous ^{1}H and ^{19}F decoupling is shown on *Figure 2d*[22]. The ^{13}C–^{19}F dipolar couplings are not suppressed by irradiation under the recording conditions of *Figure 2c*; they are only partly averaged by magic-angle spinning and therefore only a partly resolved CH_2 carbon line can be observed in the solid-state spectrum of PVF_2.

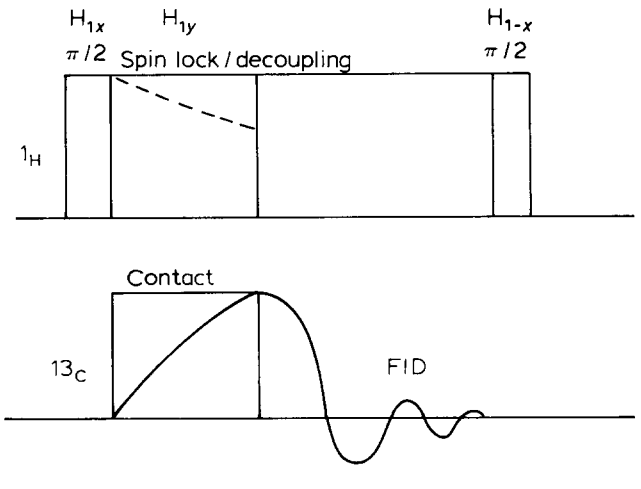

Figure 1 The cross-polarization pulse sequence used in the experiments

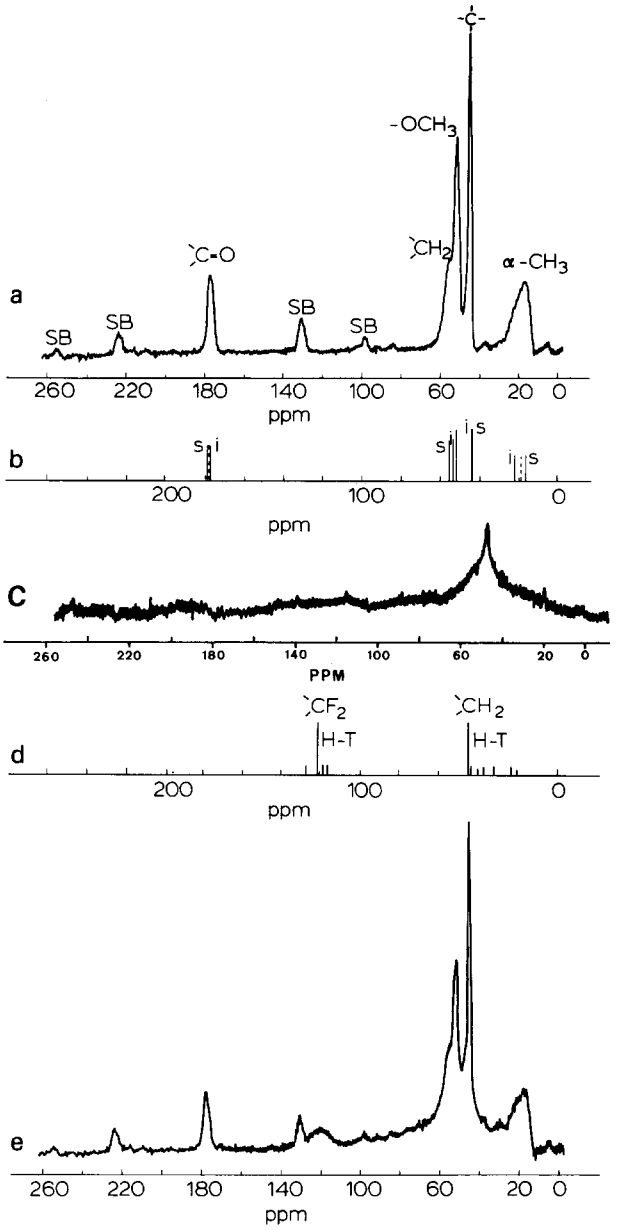

Figure 2 (a) ^{13}C CP/DD/MAS n.m.r. spectrum of solid PMMA at room temperature. (b) Stick ^{13}C n.m.r. spectrum of PMMA in solution: i, s: (———) isotactic and syndiotactic dyad or triad resonances; (– – –) heterotactic triad resonance[19–21]. (c) ^{13}C CP/DD/MAS n.m.r. spectrum of PVF_2 in bulk recorded without ^{19}F decoupling at room temperature. (d) Stick ^{13}C spectrum of PVF_2 in solution obtained with simultaneous decoupling of ^{1}H and ^{19}F nuclei; H–T: head-to-tail sequences[22]. (e) ^{13}C CP/DD/MAS n.m.r. spectrum of 70/30 PVF_2/PMMA blend at room temperature

A typical ^{13}C CP/DD/MAS n.m.r. spectrum of a PVF_2/PMMA blend is plotted in *Figure 2e*. The spectrum is not very different from that for pure PMMA shown in *Figure 2a*. Due to partial superposition of resonance signals of the methylene carbon of PVF_2 and the methylene group, ester–methyl and quaternary carbons of PMMA, the corresponding group of signals is broadened at the bottom. Analysis of isotropic chemical shifts indicates variation of the carboxyl and α-CH_3 resonances of about 0.7 ppm between the pure PMMA and the 50/50 blend spectra. This chemical shift variation is very weak.

However, since it is a monotonous function of the composition of the blends in this range of PVF_2 contents, and because of the sensitivity of the 75 MHz ^{13}C experiment, it appears significant. For amorphous compounds, isotropic ^{13}C chemical shifts arise from shielding effects that extend to no more than 10 Å[23]. Therefore, the small observed chemical shift variation between pure PMMA and PMMA incorporated in a blend may be considered as a first indication that mixing in PVF_2/PMMA blends takes place on a molecular level. Chemical shift changes may be induced either by direct interchain shielding or by indirect conformationally induced effects.

Cross-polarization experiments on quenched and annealed samples

The variation of PMMA carbon magnetization as a function of the contact duration between the ^1H and ^{13}C reservoirs in quenched samples of pure PMMA and of blends of various composition is shown in *Figure 3*. As pointed out in the introduction, it leads to the determination of the relaxation time $T_{1\rho}$ for protons attached to chemically different carbons. However, because of spin-diffusion phenomena, these times are considerably averaged and differences in the values obtained from the various carbon lines of one given sample are lower than 20% in pure PMMA as well as in PMMA blends. Additionally, all the carbons of PMMA show identical trends in their relaxation time dependence on composition ratio and thermal treatment.

For pure PMMA, 40/60 and 50/50 blends, the carbon magnetization is an exponentially decreasing function of the contact time, over the whole range of contact times investigated. Moreover the relaxation time $T_{1\rho}$, which is equal to 13.4, 6.0, and 3.7 ms for pure PMMA, 40/60 and 50/50 PVF_2/PMMA blends respectively, is a decreasing function of the PVF_2 content in these samples. The fact that only a single $T_{1\rho}$ is observed in these blends leads us to the immediate conclusion that PMMA does not form occlusions or domains in the amorphous phase of PVF_2. In either event, a $T_{1\rho}$ relaxation plot, or component of a relaxation plot, characteristic of pure PMMA would be observed. On the contrary, however, within the spatial scale of the experiment, the blends appear to be homogeneous. The decrease of the relaxation time $T_{1\rho}$ as a function of the PVF_2 content suggests either that mixing is intimate enough so that PMMA relaxation is aided by interaction with nearby, efficiently relaxing PVF_2, or that molecular motions are altered by blending. $T_{1\rho}$ relaxation for ^1H resonance in pure PMMA in a radiofrequency field of 25 Gauss have been measured by Douglass and McBrierty as a function of temperature[9]. The 12 Gauss $T_{1\rho}$ behaviour is expected to be very similar, except for a shift of a few degrees of the $T_{1\rho}$ curve towards a lower temperature. The lowering of the glass transition temperature observed in the 40/60 and 50/50 blends[12] should result in a more substantial shift of this curve towards a lower temperature. Using reported data[9] and taking into account these two shifts, allows us to conclude that in such blends at room temperature $T_{1\rho}$ is a decreasing function of temperature and therefore should decrease when the PVF_2 content increases. However, whatever the main cause of the $T_{1\rho}$ decrease in the blends: interaction with nearby PVF_2 nuclei or increasing mobility of PMMA in the blend, one is drawn to the

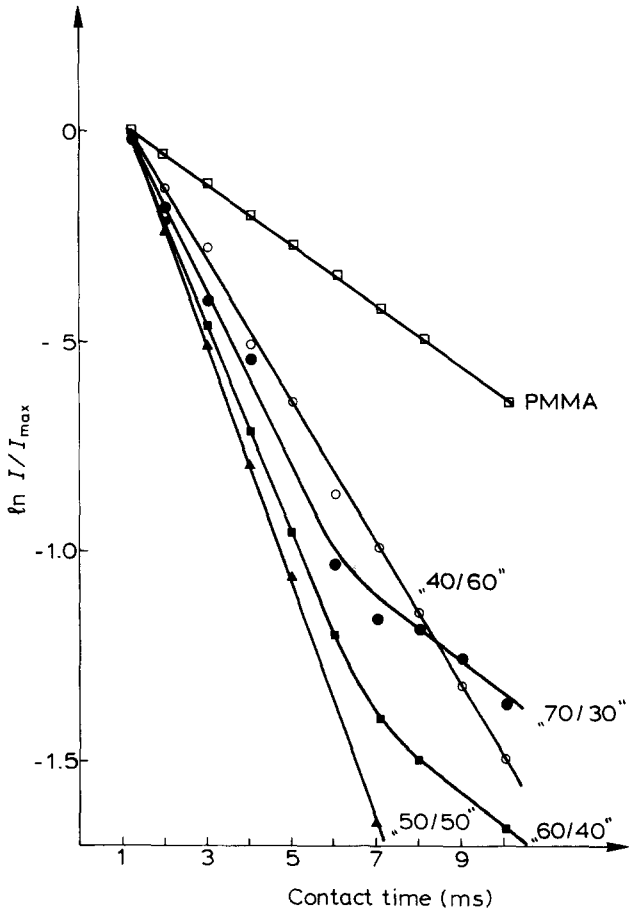

Figure 3 Plots of PMMA carbon magnetization vs. cross-polarization contact time for pure PMMA (□) and quenched PVF_2/PMMA blends with weight ratios of 40/60 (○), 50/50 (▲), 60/40 (■) and 70/30 (●)

conclusion that in the 40/60 and 50/50 blends, PMMA protons have either direct dipole interaction with PVF_2 nuclei or have sufficient PVF_2 near-neighbours to alter the PMMA dynamics. In both cases this conclusion which is that of an intimate mixing is in agreement with results derived by Douglas and McBrierty[9] from cross-relaxation measurements which have pointed out the fact that a substantial number of amorphous PVF_2 molecules see PMMA molecules at nearest neighbour distances.

As shown in *Figure 3*, the behaviour of blends possessing a higher content of PVF_2 is quite different from that observed in the 40/60 and 50/50 blends. The magnetization variation presents a double-stage character as a function of contact time. For long contact times, its dependence in the 60/40 and 70/30 PVF_2/PMMA blends is quite close to that of pure PMMA, indicating that for long contact times the magnetization arises from domains where PMMA is either pure or surrounded by only a few PVF_2 chains.

Under the assumption of a spin-diffusion relaxation mechanism, the maximum diffusive path length $\langle r \rangle$ may be estimated from the approximate formula[24]:

$$\langle r \rangle = (6DT_{1\rho})^{1/2}$$

Typically, the spin-diffusion coefficient is 10^{-12} cm^2 s^{-1}, and therefore for $T_{1\rho} \sim 10^{-2}$ s, one gets $\langle r \rangle \sim 20$ Å. Thus, it may be concluded that aggregates of rejected PMMA in 60/40 and 70/30 PVF_2/PMMA blends have linear dimensions larger than 20 Å.

The latter results can be interpreted as resulting from partial crystallization of PVF_2. On *Figure 4* is shown the variation of the degree of crystallinity of the samples under study determined by the method described in ref. 12. Comparison of *Figures 3* and *4* clearly shows that purely exponential variation of carbon magnetization and therefore intimate mixing of PVF_2 and PMMA chains do occur for amorphous samples (40/60 and 50/50 PVF_2/PMMA blends), whereas for partly crystalline blends (60/40 and 70/30 PVF_2/PMMA blends) the decrease of carbon magnetization presents a two-step character. Besides, the relaxation time $T_{1\rho}$ in the 40/60 and 50/50 PVF_2/PMMA blends as well as the initial relaxation time $T_{1\rho}$ in the 60/40 and 70/30 PVF_2/PMMA blends are clearly related to the composition of the amorphous phase. It must be pointed out that, in the 60/40 and 70/30 PVF_2/PMMA blends, the composition of the amorphous phase is richer in PMMA than that of the whole sample as a result of partial crystallization of PVF_2 chains. The long time relaxation rate observed in the latter samples and reflecting domains where PMMA is either pure or surrounded by only a few PVF_2 chains is a consequence of the crystallization process. Indeed, due to PVF_2 crystallization during sample quenching, the chains of PMMA that are intermixed before crystallization occurs, are rejected from the crystalline regions. Thus, in the amorphous region next to the growing crystals, this leads temporarily to domains with a much higher content of PMMA chains, as compared with the intimate mixing of the bulk amorphous phase. Following this scheme, for annealed samples, as diffusion may occur, re-equilibration of PMMA distribution in the amorphous phase should happen as a consequence of the compatibility of PVF_2/PMMA blends.

To test this assumption of the molecular origin of the PMMA chain rejection, experiments have been performed on annealed samples. 60/40 and 70/30 PVF_2/PMMA blends were annealed for one hour at 373 K. The dependence of ^{13}C magnetization as a function of contact time for these annealed samples is plotted in *Figure 5*. Indeed, in comparison with *Figure 3*, the break of line in the magnetization variation is less pronounced here.

Additional arguments justifying our interpretation can

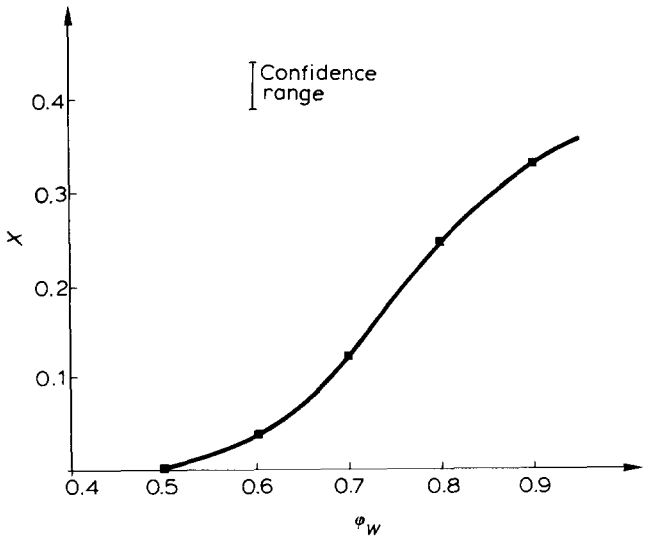

Figure 4 Degree of crystallinity X vs. PVF_2 weight fraction is quenched PVF_2/PMMA blends

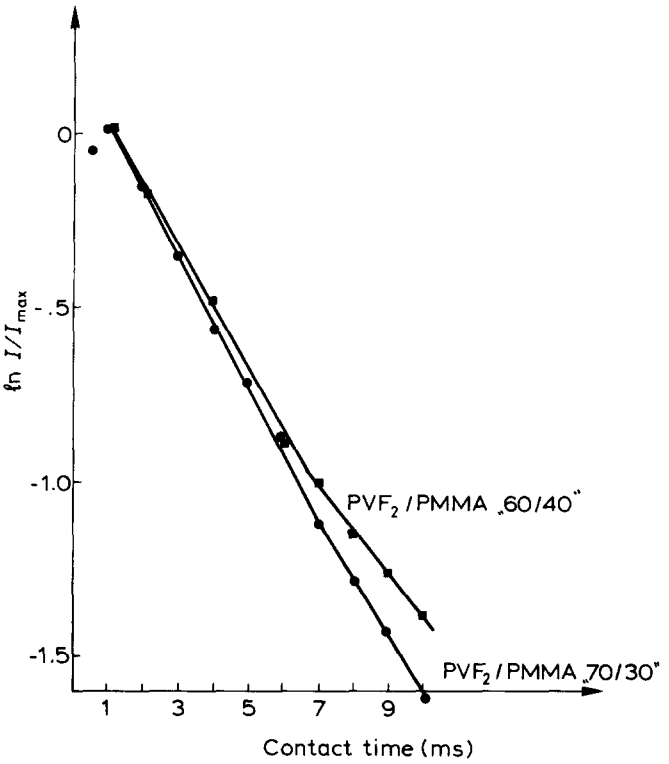

Figure 5 Plots of PMMA carbon magnetization vs. cross-polarization contact time for 60/40 (■) and 70/30 (●) PVF_2/PMMA blends annealed for one hour at 373 K

be found in two other sets of experiments on a 50/50 blend which can either be obtained in an amorphous state or it can be crystallized. In *Figure 6*, the variations of carbon magnetization as a function of the contact time for quenched (amorphous) 50/50 sample and for 50/50 blends cooled from 463 K to room temperature at cooling rates of 0.2 degrees/min and 10 degrees/min are plotted. In the case of the blend cooled with a cooling rate of 0.2 degrees/min, the carbon magnetization is an exponential function of the contact time, which indicates an intimate mixing of all the PMMA chains of the sample, and the relaxation rate is slower than in the quenched blend which is evidence for an amorphous phase richer in PMMA than that of the quenched sample. These conclusions are in total agreement with the expected situation, namely that, thanks to the slow cooling rate used in this experiment, re-equilibration of the PMMA chains in the amorphous phase of the blend is complete. With a faster cooling rate of 10 degrees/min, diffusion of PMMA rejected from crystalline PVF_2 regions is not efficient enough for the above complete re-equilibration, and thus a break in the magnetization decay is observed, pointing out the presence of two kinds of PMMA chains in the sample: (1) intimately mixed PMMA segments in the bulk emorphous phase and (2) rejected PMMA chains at the crystallization front. It should be noted that yt the relaxation rate at long contact times differs from that of pure PMMA. This fact can be interpreted in terms of PVF_2 and PMMA diffusion processes at the crystallization front which, though not completed, lead to an already PVF_2 enriched PMMA phase at the crystallization front.

In the second set of experiments on the 50/50 blend, the samples have been heated to 358 K with a heating rate of 10 degrees/min and additionally annealed at this temperature for different time periods ranging from 15

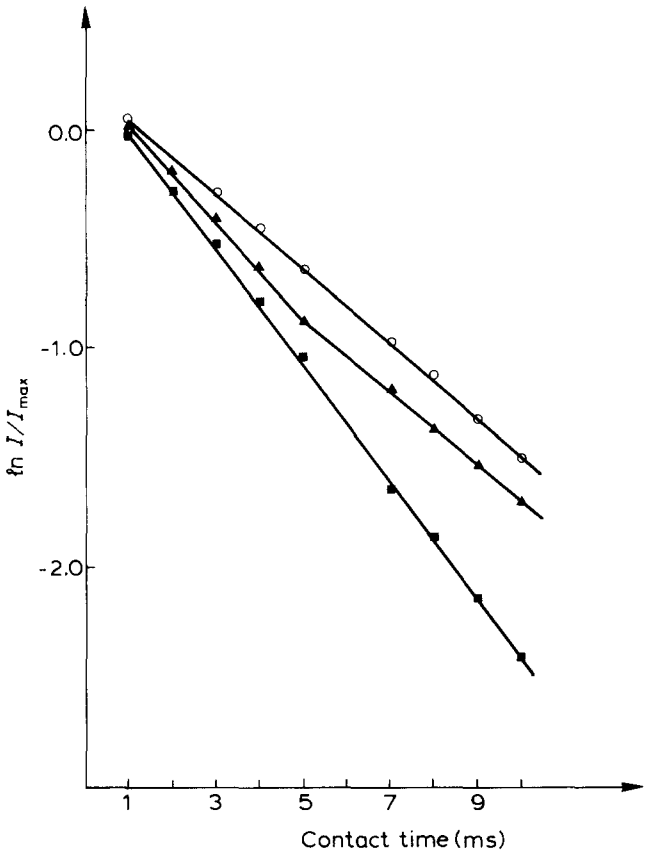

Figure 6 Plots of PMMA carbon magnetization vs. cross-polarization contact time for quenched 50/50 PVF_2/PMMA blend (■) and for 50/50 PVF_2/PMMA cooled from 463 K to room temperature at cooling rates of 0.2 degrees/min (○) and 10 degrees/min (▲)

min to 8 h. The degrees of crystallinity of these samples, as a function of the annealing duration, are given in *Table 1*. The effect of such a thermal treatment on the variation of the magnetization as a function of the contact time is shown in *Figure 7*. The magnetization decay observed for the 8 h annealing time is strictly exponential and presents a relaxation rate slower than that of the quenched 50/50 blend. The interpretation of this result is similar to that given for the slowly cooled 50/50 blend. In both cases thermal treatment is such that complete re-equilibration of the amorphous phase takes place. For samples annealed for 1 and 2 h, the re-equilibration is not completed. The shapes of the magnetization decays in these two samples are very similar, which is in agreement with the establishment of a stationary regime at the crystallization front. The variation of the carbon magnetization in the 15 min annealed sample is strictly exponential and, though faster than the relaxation rate of the 8 h annealed sample, its relaxation rate is slower than that of the quenched blend. This result is consistent with the values of the degree of crystallinity of these samples reported in *Table 1* and indicates that, after such a period of time, the crystalline phase is mainly made of nuclei and lamellae of small dimensions so that the PMMA domains which are rejected at the borders of the crystalline domains have linear dimensions less than 20 Å.

Summing up, it can be stated that, as shown by the above study of PVF_2/PMMA blends, the cross-polarization experiment based on the observation of a proton reservoir in the rotating frame via magnetization of carbon nuclei, performed on quenched and annealed

Table 1 Degree of crystallinity (X) of 50/50 PVF_2/PMMA blend as a function of annealing duration. Determinations have been carried out according to ref. 12.

t (min)	15	60	120	480
X (%)	7	12	14	15

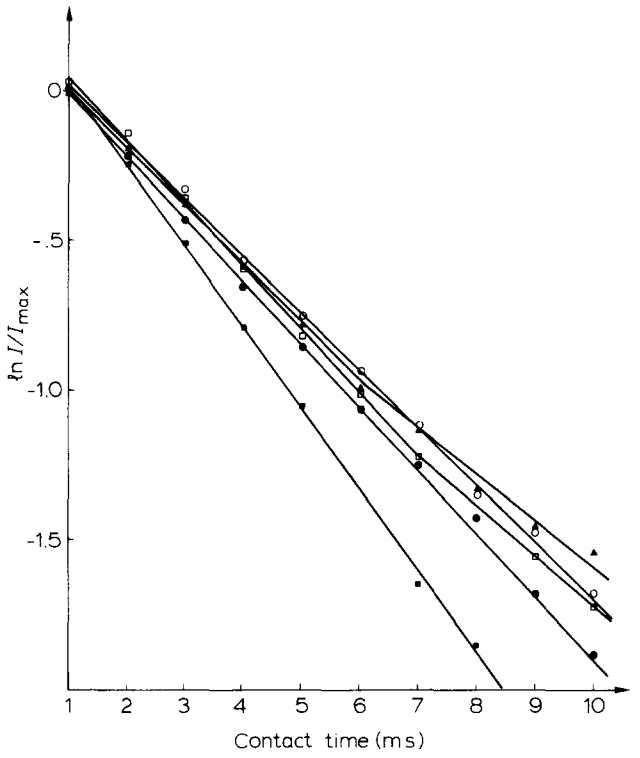

Figure 7 Plots of PMMA carbon magnetization vs. cross-polarization contact time for 50/50 PVF_2/PMMA quenched sample (■) and samples annealed at 358 K for 15 min (●), 1 h (□), 2 h (▲) and 8 h (○)

blends, is very sensitive to composition, crystallization induced morphological changes and thermal history of the samples. It provides a powerful tool for studying heterogeneities on a molecular level and furthermore it seems possible, from a calibration obtained from amorphous blends of various compositions, to achieve a precise determination of composition of the amorphous phase.

ACKNOWLEDGEMENTS

The authors thank Drs J. L. Halary and C. Leonard for many helpful discussions and suggestions.

The support of this study by the 'Centre National de la Recherche Scientifique' under contract No. ATP 983004 is appreciated.

REFERENCES

1 Noland, J. S., Hsu, N. N. C., Saxon, R. and Schmitt, J. M. *Adv. Chem. Ser.* 1971, **99**, 1
2 Nishi, T. and Wang, T. T. *Macromolecules* 1975, **8**, 909
3 Aubin, M. and Prud'homme, R. E. *J. Polym. Sci., Polym. Phys. Edn.* 1981, **19**, 1245
4 Roerdink, E. and Challa, G. *Polymer* 1978, **19**, 173
5 Hourston, O. J. and Hughes, I. D. *Polymer* 1977, **18**, 1175
6 Morra, B. S. *Ph. D. Thesis*, University of Massachusetts, 1980
7 Coleman, M. M., Zarian, J., Varnell, D. F. and Painter, P. C. *J. Polym. Sci., Polym. Lett. Edn.* 1977, **15**, 745

8 Wendorff, J. H. *J. Polym. Sci., Polym. Lett. Edn.* 1980, **18**, 439
9 Douglass, D. C. and McBrierty, V. J. *Macromolecules* 1978, **11**, 766
10 Lin, T. S. and Ward, T. C. *ACS Polymer Prepr.* 1983, **24**, 136
11 Khambatta, F. B., Warner, F., Russel, T. and Stein, R. S. *J. Polym. Sci., Polym. Phys. Edn.* 1976, **14**, 1391
12 Leonard, C., Halary, J. L., Monnerie, L., Broussoux, D., Servet, B. and Micheron, F. *Polymer* 1983, **24**, (*Commun.*) 110
13 Stejskal, E. O., Schaefer, J., Sefcik, M. D. and McKay, R. A. *Macromolecules* 1981, **14**, 275
14 Schaefer, J., Sefcik, M. D., Stejskal, E. O. and McKay, R. A. *Macromolecules* 1981, **14**, 188
15 Schaefer, J., Stejskal, E. O. and Buchdahl, R. *Macromolecules* 1977, **10**, 384
16 Schaefer, J., Stejskal, E. O., Sefcik, M. D. and McKay, R. A. *Phil. Trans. Roy. Soc. Lond. A* 1981, **299**, 593
17 Stejskal, E. D. and Schaefer, J. *J. Magn. Reson.* 1975, **18**, 560
18 Tegenfelft, J., Haeberlen, U. and Waugh, J. S. *J. Magn. Reson.* 1979, **36**, 453
19 Peat, I. R. and Reynolds, W. F. *Tetrahedron Lett.* 1972, **14**, 1359
20 Lyerla, J. R., Horikawa, T. T. and Johnson, D. E. *J. Am. Chem. Soc.* 1977, **99**, 2463
21 Edzes, H. T. and Veeman, W. S. *Polym. Bull.* 1981, **5**, 255
22 Tonelli, A. E., Schilling, F. C. and Cais, R. E. *Macromolecules* 1981, **14**, 560
23 Tonelli, A. E. *Macromolecules* 1979, **12**, 255
24 McBrierty, V. J., Douglass, D. C., Kwei, T. W. *Macromolecules* 1978, **11**, 1265